Heavy Physics Contributions to Neutrinoless Double Beta Decay from QCD

A. Nicholson,[1,2,*] E. Berkowitz,[3] H. Monge-Camacho,[4,5] D. Brantley,[4,6,5] N. Garron,[7] C. C. Chang,[8,2,5] E. Rinaldi,[9,5] M. A. Clark,[10] B. Joó,[11] T. Kurth,[12] B. C. Tiburzi,[13,14] P. Vranas,[6,5] and A. Walker-Loud[5,6,2]

[1]*Department of Physics and Astronomy, University of North Carolina, Chapel Hill, North Carolina 27516-3255, USA*
[2]*Department of Physics, University of California, Berkeley, California 94720, USA*
[3]*Institut für Kernphysik and Institute for Advanced Simulation, Forschungszentrum Jülich, 54245 Jülich, Germany*
[4]*Department of Physics, The College of William & Mary, Williamsburg, Virginia 23187, USA*
[5]*Nuclear Science Division, Lawrence Berkeley National Laboratory, Berkeley, California 94720, USA*
[6]*Physics Division, Lawrence Livermore National Laboratory, Livermore, California 94550, USA*
[7]*Theoretical Physics Division, Department of Mathematical Sciences, University of Liverpool, Liverpool L69 3BX, United Kingdom*
[8]*Interdisciplinary Theoretical and Mathematical Sciences Program (iTHEMS), RIKEN 2-1 Hirosawa, Wako, Saitama 351-0198, Japan*
[9]*RIKEN-BNL Research Center, Brookhaven National Laboratory, Upton, New York 11973, USA*
[10]*NVIDIA Corporation, 2701 San Tomas Expressway, Santa Clara, California 95050, USA*
[11]*Scientific Computing Group, Thomas Jefferson National Accelerator Facility, Newport News, Virginia 23606, USA*
[12]*NERSC Lawrence Berkeley National Laboratory, Berkeley, California 94720, USA*
[13]*Department of Physics, The City College of New York, New York, New York 10031, USA*
[14]*Graduate School and University Center, The City University of New York, New York, New York 10016, USA*

(Received 16 May 2018; published 25 October 2018)

Observation of neutrinoless double beta decay, a lepton number violating process that has been proposed to clarify the nature of neutrino masses, has spawned an enormous world-wide experimental effort. Relating nuclear decay rates to high-energy, beyond the standard model (BSM) physics requires detailed knowledge of nonperturbative QCD effects. Using lattice QCD, we compute the necessary matrix elements of short-range operators, which arise due to heavy BSM mediators, that contribute to this decay via the leading order $\pi^- \to \pi^+$ exchange diagrams. Utilizing our result and taking advantage of effective field theory methods will allow for model-independent calculations of the relevant two-nucleon decay, which may then be used as input for nuclear many-body calculations of the relevant experimental decays. Contributions from short-range operators may prove to be equally important to, or even more important than, those from long-range Majorana neutrino exchange.

DOI: 10.1103/PhysRevLett.121.172501

Introduction.—Neutrinoless double beta decay ($0\nu\beta\beta$) is a process that, if observed, would reveal violations of symmetries fundamental to the standard model and would guarantee that neutrinos have nonzero Majorana mass [1,2]. Such decays can probe physics beyond the electroweak scale and expose a source of lepton number (L) violation that may explain the observed matter-antimatter asymmetry in the Universe [3,4]. Existing and planned experiments will constrain this novel nuclear decay [5–16], but the interpretation of the resulting decay rates or limits as constraints on new physics poses a tremendous theoretical challenge.

The most widely discussed mechanism for $0\nu\beta\beta$ is that of a light Majorana neutrino, which can propagate a long distance within a nucleus. However, if the mechanism involves a heavy scale $\Lambda_{\beta\beta}$, the resulting L-violating process can be short ranged. While naïvely short-range operators are suppressed compared to long-range interactions, due to the heavy mediator propagator, in the case of $0\nu\beta\beta$, the long-range interaction requires a helicity flip and is proportional to the mass of the light neutrino. In a standard seesaw scenario [17–21], this light neutrino mass is similarly suppressed by the same large mass scale, so the relative importance of long- versus short-range contributions is dependent upon the particle physics model under consideration and, in general, cannot be determined until the nuclear matrix elements for both types of processes are computed.

Both long- and short-range mechanisms present substantial theoretical challenges if we hope to connect high-energy physics with experimentally observed decay rates. The former case is difficult because one must understand long-distance nuclear correlations. In the latter case, the short-distance physics is masked by QCD effects, requiring nonperturbative methods to match few-nucleon matrix elements to standard model operators.

Effective field theory (EFT) arguments show that, at leading order (LO) in the standard model, there are nine local four-quark operators that can contribute to $0\nu\beta\beta$ decays [22,23]. Further matching to a nuclear EFT [22] shows that, at lowest order, there are up to three important processes—a negatively charged pion in the nucleus can be converted to a positively charged pion, releasing two electrons ($\pi\pi ee$ operators), a neutron can be converted

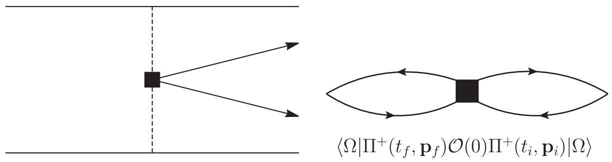

FIG. 1. (Left) The leading order contribution to $0\nu\beta\beta$ via short-range operators occurs within a long-distance pion-exchange diagram. The nucleons (solid lines) exchange charged pions (dashed), which emit two electrons (lines with arrowheads). (Right) The LECs associated with the operators in the left panel may be calculated through a simpler $\pi^-\to\pi^+$ transition. Here, the lines represent quarks.

to a proton plus a positively charged pion, also releasing two electrons ($NN\pi ee$ operators), and finally, two neutrons can be converted to two protons plus two electrons ($NNNNee$ operators). As long as the LO $\pi\pi ee$ operators are not forbidden by symmetries, the LO contribution to the nuclear $0\nu\beta\beta$ transition matrix element in the Weinberg counting scheme [24,25] will be given by the $\pi\pi ee$ operators within the pion-exchange diagram shown in the left panel of Fig. 1. More recent EFT analyses for operators relevant to $0\nu\beta\beta$ have indicated that the contact operators $NNNNee$ may be enhanced, in which case they would also appear at LO [26].

In this Letter, we determine the matrix elements of the relevant $\pi\pi ee$ operators and their associated low-energy constants (LECs) for chiral perturbation theory (χPT) using lattice QCD (LQCD), a nonperturbative numerical method with fully controllable systematics. We perform extrapolations in all parameters characterizing deviations from the physical point, including quark mass and lattice spacing a, which controls effects from the discretization of space and time.

Method.—Using the EFT framework, it is not necessary to calculate the full $nn\to ppee$ transition shown in the left panel of Fig. 1. Instead, we can perform the much more computationally tractable calculation of the on shell $\pi^-\to\pi^+$ transition in the presence of external currents (four-quark operators). Once the LECs are determined, calculating the true off shell process can be dealt with naturally within the EFT framework. From a LQCD perspective, this single pion calculation is computationally far simpler than the two-nucleon calculation due to the absence of a signal-to-noise problem [27] and complications in accounting for scattering states in a finite volume [28,29].

We calculate matrix elements for the following relevant four-quark operators described in Ref. [22]:

$$\begin{aligned}
\mathcal{O}_{1+}^{++} &= (\bar{q}_L\tau^+\gamma^\mu q_L)[\bar{q}_R\tau^+\gamma_\mu q_R],\\
\mathcal{O}_{2+}^{++} &= (\bar{q}_R\tau^+ q_L)[\bar{q}_R\tau^+ q_L] + (\bar{q}_L\tau^+ q_R)[\bar{q}_L\tau^+ q_R],\\
\mathcal{O}_{3+}^{++} &= (\bar{q}_L\tau^+\gamma^\mu q_L)[\bar{q}_L\tau^+\gamma_\mu q_L]\\
&\quad + (\bar{q}_R\tau^+\gamma^\mu q_R)[\bar{q}_R\tau^+\gamma_\mu q_R],
\end{aligned}\tag{1}$$

where the Takahashi bracket notation () or [] indicates which color indices are contracted together [30]. We have omitted parity odd operators that do not contribute to the $\pi^-\to\pi^+$ transition, as well as the vector operators that are suppressed by the electron mass, as discussed in Ref. [22]. In addition, we calculate the color-mixed operators that arise through renormalization from the electroweak scale to the QCD scale [23],

$$\begin{aligned}
\mathcal{O}_{1+}^{\prime++} &= (\bar{q}_L\tau^+\gamma^\mu q_L][\bar{q}_R\tau^+\gamma_\mu q_R),\\
\mathcal{O}_{2+}^{\prime++} &= (\bar{q}_L\tau^+ q_L][\bar{q}_L\tau^+ q_L) + (\bar{q}_R\tau^+ q_R][\bar{q}_R\tau^+ q_R).
\end{aligned}\tag{2}$$

The analogous color-mixed operator $\mathcal{O}_{3+}^{\prime++}$ is identical to $\mathcal{O}_{3+}^{++}$ and is therefore omitted.

To determine the matrix elements for the $\pi\pi ee$ operators, we have performed a LQCD calculation using the publicly available highly improved staggered quark (HISQ) [31] gauge field configurations generated by the MILC collaboration [32,33]. The set of configurations used is shown in Table I. With this set, we perform extrapolations in the lattice spacing, pion mass, and volume. On these configurations, we chose to produce Möbius domain wall quark propagators [34–36] due to their improved chiral symmetry properties, which suppress mixing between operators of different chirality. To further improve the chiral properties, we first performed a gradient flow method to smooth the HISQ configurations [37–39] (see Ref. [40] for details). This action has been successfully used to compute the nucleon axial coupling g_A with 1% precision [41–43]. For each ensemble, we have generated quark propagators using both wall and point sources on approximately 1000 configurations.

The calculation of the matrix elements proceeds along the same lines as calculations of K^0 [44–52], D^0 [50,53], and $B_{(s)}^0$ meson mixing [54–57] or $N\bar{N}$ oscillations [58–60] and involves only a single light quark inversion from an unsmeared point source at the time where the four-quark operator insertion occurs. The propagators are then contracted to produce a pion at an earlier time (source) and later time (sink). Because no quark propagators connect the source to the sink, we can exactly project both source and

TABLE I. List of HISQ ensembles used for this calculation, showing the volumes ($V=L^3\times T$) studied for a given lattice spacing and pion mass.

	$m_\pi\sim 310$ MeV		$m_\pi\sim 220$ MeV		$m_\pi\sim 130$ MeV	
a(fm)	V	$m_\pi L$	V	$m_\pi L$	V	$m_\pi L$
0.15	$16^3\times 48$	3.78	$24^3\times 48$	3.99		
0.12			$24^3\times 64$	3.22		
0.12	$24^3\times 64$	4.54	$32^3\times 64$	4.29	$48^3\times 64$	3.91
0.12			$40^3\times 64$	5.36		
0.09	$32^3\times 96$	4.50	$48^3\times 96$	4.73		

sink onto definite momentum (allowing only zero momentum transfer at the operator) without the use of all-to-all propagators.

Results.—In Fig. 2, we show representative plots on the near-physical pion mass ensemble ($V = 48^3 \times 64$, $a = 0.12$ fm, $m_\pi \sim 130$ MeV), of the ratio

$$\mathcal{R}_i(t) \equiv C_i^{3\mathrm{pt}}(t, T-t)/[C_\pi(t)C_\pi(T-t)], \tag{3}$$

where $C_i^{3\mathrm{pt}}$ is the three-point function with a four-quark operator labeled by i at $t = 0$ and the sink (source) at time $t_f = t$ ($t_i = T - t$),

$$C_i^{3\mathrm{pt}}(t_f, t_i) = \sum_{\mathbf{x},\mathbf{y},\alpha} \langle \alpha | \Pi^+(t_f, \mathbf{x}) \mathcal{O}_i(0, \mathbf{0}) \Pi^+(t_i, \mathbf{y}) | \alpha \rangle e^{-E_\alpha T} \tag{4}$$

where α labels QCD eigenstates, and the pion interpolating field is $\Pi^+ = (\Pi^-)^\dagger = \bar{d}\gamma_5 u$. C_π is the pion correlation function. Using relativistic normalization,

$$\begin{aligned} C_\pi(t) &= \sum_{\mathbf{x}} \sum_\alpha \langle \alpha | \Pi^+(t, \mathbf{x}) \Pi^-(0, \mathbf{0}) | \alpha \rangle e^{-E_\alpha T} \\ &= \sum_n \frac{|Z_n^\pi|^2}{2E_n^\pi} (e^{-E_n^\pi t} + e^{-E_n^\pi (T-t)}) + \cdots, \end{aligned} \tag{5}$$

where $Z_n^\pi = \langle \Omega | \Pi^+ | n \rangle$, Ω represents the QCD vacuum, and the ellipses represent thermally suppressed terms. One can show that the ratio correlation function is given in lattice units by

$$\mathcal{R}_i(t) = \frac{a^4 \langle \pi | \mathcal{O}_{i+}^{++} | \pi \rangle}{(a^2 Z_0^\pi)^2} + \mathcal{R}_{\mathrm{ES}}(t), \tag{6}$$

where $|\pi\rangle$ is the ground state pion and the excited state (ES) contributions are suppressed exponentially by their mass gap relative to the pion mass, $\mathcal{R}_{\mathrm{ES}}(t) \propto e^{-(E_n^\pi - E_0^\pi)t}$. The overlap factors Z_π^0 are determined in the analysis of the two-point pion correlation functions. For brevity we henceforth write the matrix elements of these operators as $O_i = \langle \pi | \mathcal{O}_{i+}^{++} | \pi \rangle$ and attach a prime as appropriate.

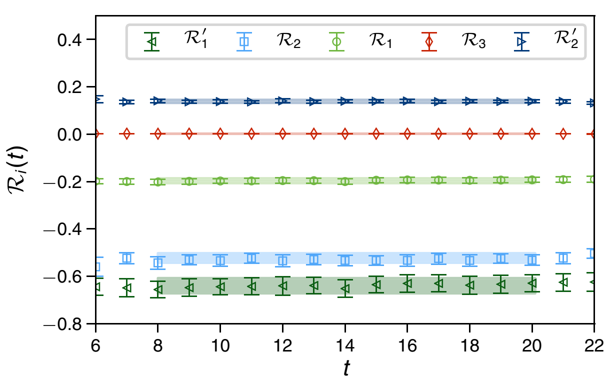

FIG. 2. An example of our lattice results for different operators on the near-physical pion mass ensemble with $a \simeq 0.12$ fm.

We find excellent signals on nearly all ensembles, requiring only a simple fit to a constant. This is likely due to the fact that, in the ratio defined in Eq. (3), the contribution from the lowest thermal pion state is eliminated, which we find to be the leading contamination to the pion correlation function within the relevant time range. We also find little variation of the ratio using either wall or point sources. This gives us additional confidence that excited state contamination is negligible within the time range plotted in the left panel of Fig. 2. A preliminary version of this analysis was presented in Ref. [61]. Excited state contamination is studied further in the Supplemental Material [62].

After extracting the matrix elements on each ensemble, we perform extrapolations to the continuum, physical pion mass, and infinite volume limits. It is straightforward to include these new operators in χPT [84] and to derive the virtual pion corrections that arise at next-to-leading order (NLO) in the chiral expansions,

$$\begin{aligned} O_1 &= \frac{\beta_1 \Lambda_\chi^4}{(4\pi)^2}(1 + \epsilon_\pi^2[\ln(\epsilon_\pi^2) - 1 + c_1]), \\ O_2 &= \frac{\beta_2 \Lambda_\chi^4}{(4\pi)^2}(1 + \epsilon_\pi^2[\ln(\epsilon_\pi^2) - 1 + c_2]), \\ \frac{O_3}{\epsilon_\pi^2} &= \frac{\beta_3 \Lambda_\chi^4}{(4\pi)^2}(1 - \epsilon_\pi^2[3\ln(\epsilon_\pi^2) + 1 - c_3]), \end{aligned} \tag{7}$$

as described in some detail in the Supplemental Material [62]. In these expressions,

$$\Lambda_\chi = 4\pi F_\pi, \qquad \epsilon_\pi = \frac{m_\pi}{\Lambda_\chi}, \tag{8}$$

where $F_\pi = F_\pi(m_\pi)$ is the pion decay constant at a given pion mass, normalized to be $F_\pi^{\mathrm{phys}} = 92.2$ MeV at the physical pion mass, Λ_χ is the chiral symmetry breaking scale and ϵ_π^2 is the small expansion parameter for χPT. The pion matrix elements for $\mathcal{O}_{1+}'^{++}$ and $\mathcal{O}_{2+}'^{++}$ have an identical form to $\mathcal{O}_{1+}^{++}$ and $\mathcal{O}_{2+}^{++}$, respectively, but have independent LECs β_i' and c_i', which describe the pion mass dependence. These expressions can be generalized to incorporate finite lattice spacing corrections [85] arising from the particular lattice action we have used [40] and finite volume corrections [86], which arise from virtual pions that are sensitive to the finite periodic volume used in the calculations. Details of the derivation of the formula in χPT and the extension to incorporate these lattice QCD systematic effects are presented in the Supplemental Material [62]. In addition to the matrix elements O_i, the various LECs β_i and c_i are determined in this Letter.

TABLE II. Resulting matrix elements extrapolated to the physical point, renormalized in RI/SMOM and $\overline{\mathrm{MS}}$, both at $\mu = 3$ GeV.

$O_i[\mathrm{GeV}]^4$	RI/SMOM $\mu = 3$ GeV	$\overline{\mathrm{MS}}$ $\mu = 3$ GeV
O_1	$-1.91(13) \times 10^{-2}$	$-1.89(13) \times 10^{-2}$
O_1'	$-7.22(49) \times 10^{-2}$	$-7.81(54) \times 10^{-2}$
O_2	$-3.68(31) \times 10^{-2}$	$-3.77(32) \times 10^{-2}$
O_2'	$1.16(10) \times 10^{-2}$	$1.23(11) \times 10^{-2}$
O_3	$1.85(10) \times 10^{-4}$	$1.86(10) \times 10^{-4}$

The lattice QCD results are renormalized nonperturbatively following the Rome-Southampton method [87] with a nonexceptional kinematics-symmetric point [88]. More precisely, we compute the relevant Z matrix in the RI/SMOM (γ_μ, γ_μ) scheme [89]. We implement momentum sources [90] to achieve a high statistical precision and nonperturbative scale evolution techniques [91,92] to run the Z factors to the common scale of $\mu = 3$ GeV. Further details about the renormalization procedure are provided in the Supplemental Material [62]. One advantage of our mixed-action setup is that the renormalization pattern is the same as in the continuum (to a very good approximation) and does not require the spurious subtraction of operators of different chirality.

The renormalized operators, extrapolated to the continuum, infinite volume, and physical pion mass (defined by $m_\pi^{\mathrm{phys}} = 139.57$ MeV and $F_\pi^{\mathrm{phys}} = 92.2$ MeV) limits are given in Table II in both RI/SMOM and $\overline{\mathrm{MS}}$ schemes at $\mu = 3$ GeV. An error breakdown for the statistical and various systematic uncertainties is given in the Supplemental Material [62].

The correlation between these RI-SMOM matrix elements are given in the Supplemental Material [62]. The extrapolations of these operators to the physical point are presented in Fig. 3, with the dashed vertical line representing the physical pion mass. The small value of O_3 reflects the fact that the $\mathcal{O}_{3+}^{++}$ operator is suppressed in the chiral expansion, vanishing in the chiral limit. In addition to the full mixed-action EFT extrapolations (including infinite volume), we performed further extrapolations without including mixed-action and/or finite volume effects and found all results to be consistent, indicating that mixed-action and finite volume effects are mild. These various analysis options are all available in Ref. [93]. Loss function minimization is performed using Ref. [94].

We can compare the values of the matrix elements determined here in $\overline{\mathrm{MS}}$ to those in Ref. [95], which used SU(3) flavor symmetry to determine the values, including estimated SU(3) flavor-breaking corrections at NLO in SU(3) χPT. Noting the differences in operator definition pointed out in footnote 5 of Ref. [95], we find the values of the matrix elements tend to agree at the one- to two-sigma level, as measured by the O(20%–40%) uncertainties in

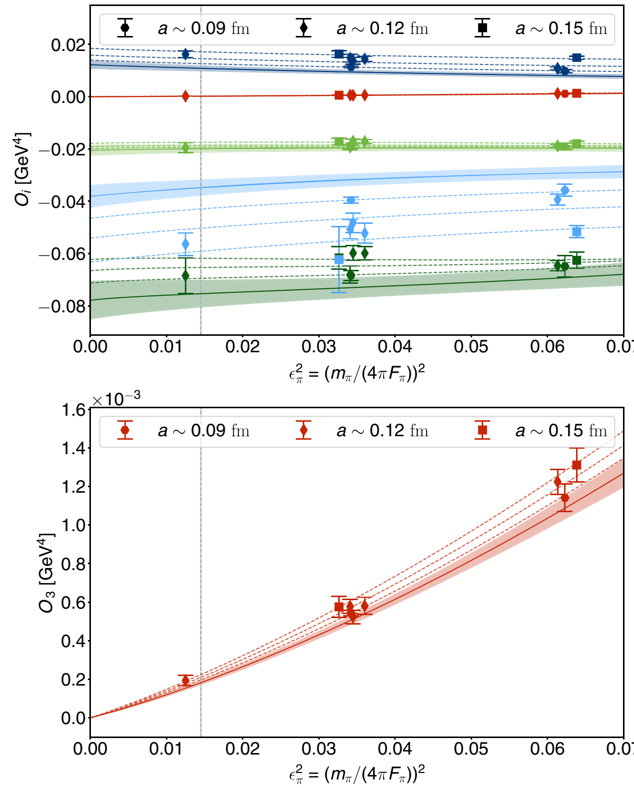

FIG. 3. The interpolation of the various matrix elements (color coded as in Fig. 2). (Bottom) Enlarged version of O_3 is displayed. The resulting fit curves and uncertainty bands are constructed with Λ_χ held fixed, while changing ϵ_π, and so the corresponding LQCD results are adjusted by $(F_\pi^{\mathrm{phys}}/F_\pi^{\mathrm{latt}})^4$ for each lattice ensemble to be consistent with this interpolation. The bands represent the 68% confidence interval of the continuum, infinite volume extrapolated value of the matrix elements. The vertical gray band highlights the physical pion mass.

Ref. [95], indicating the SU(3) chiral expansion is reasonably well behaved. With the ∼1000 measurements per ensemble in the LQCD calculation presented here, the uncertainties have been reduced to O(5%–9%). The resulting LECs are reported in Table III in the Supplemental Material [62] and the full covariance between them is provided in Ref. [93].

From the matrix element O_3 we can determine the value of B_π, the bag parameter of neutral meson mixing in the standard model, $B_\pi = O_3/[(8/3)m_\pi^2 F_\pi^2] = 0.420(23)$ [0.421(23)] in the RI/SMOM [$\overline{\mathrm{MS}}$] scheme at $\mu = 3$ GeV. This is a rather low value, indicating a large deviation from the vacuum saturation approximation. However, this is expected from the chiral behavior as discussed, for example, in Ref. [96–98]. As displayed in Fig. 5 in the Supplemental Material [62], the value of B_π increases at larger pion masses, as expected.

Discussion.—We have performed the first LQCD calculation of hadronic matrix elements for short-range operators contributing to $0\nu\beta\beta$. This calculation is complete for matrix elements contributing to leading order in χPT, including extrapolation to the physical point in both lattice spacing and pion mass. We have also performed calculations directly at the physical pion mass.

Given these $\pi^- \to \pi^+$ matrix elements, the nuclear beta decay rate can be determined by constructing the $nn \to pp$ potential that they induce. The strong contribution to this potential for the matrix elements O_i for $i = 1, 2$ is given by

$$V_i^{nn\to pp}(|\mathbf{q}|) = -O_i P_{1+} P_{2+} \frac{\partial}{\partial m_\pi^2} V_{1,2}^\pi(|\mathbf{q}|)$$
$$= -O_i \frac{g_A^2}{4F_\pi^2} \tau_1^+ \tau_2^+ \frac{\sigma_1 \cdot \mathbf{q} \sigma_2 \cdot \mathbf{q}}{(|\mathbf{q}|^2 + m_\pi^2)^2}, \qquad (9)$$

where $V_{1,2}^\pi(|\mathbf{q}|) = -\tau_1 \cdot \tau_2 \sigma_1 \cdot \mathbf{q} \sigma_2 \cdot \mathbf{q}/(|\mathbf{q}|^2 + m_\pi^2)$ is the long-range pion-exchange potential between two nucleons (labeled 1 and 2) and $P_{1,2}^+$ project onto the isospin raising operator for each nucleon. For O_3, the potential is

$$V_3^{nn\to pp}(|\mathbf{q}|) = -\frac{O_3}{m_\pi^2} \frac{g_A^2}{4F_\pi^2} \tau_1^+ \tau_2^+$$
$$\times \left(\frac{m_\pi^2 \sigma_1 \cdot \mathbf{q} \sigma_2 \cdot \mathbf{q}}{(|\mathbf{q}|^2 + m_\pi^2)^2} - \frac{\sigma_1 \cdot \mathbf{q} \sigma_2 \cdot \mathbf{q}}{|\mathbf{q}|^2 + m_\pi^2} \right), \qquad (10)$$

up to relativistic corrections. These potentials need to be multiplied by the electrons $\bar{e}e^c$, the overall prefactor $G_F^2/\Lambda_{\beta\beta}$, and the Wilson coefficient of the effective standard model operators for a given heavy physics model to determine the full $nn \to ppe^-e^-$ amplitude. These matrix elements, once incorporated into nuclear decay rate calculations, can be used to place limits on the various beyond the standard model (BSM) mechanisms that give rise to $0\nu\beta\beta$ (see, for example, [22,23,99–108]). The limits on the BSM mechanisms must also account for the running of these short-distance operators, which can modify their strength by an amount comparable to the current uncertainties on the nuclear matrix elements themselves [109].

Modern analyses use effective field theory [22,23,107,108], for which this contribution is the leading order short-range correction. To go beyond leading order in χPT, additional calculations are necessary. For planned experiments probing $0^+ \to 0^+$ nuclear transitions, all next-to-leading order diagrams of type $NN\pi ee$ vanish due to parity [22]. At next-to-next-to-leading order there exist both $NN\pi ee$ diagrams and $NNNNee$ contact diagrams. Calculation of the $NNNNee$ contact contribution may prove important, as diagrams involving light pion exchange may need to be summed nonperturbatively in the EFT framework, causing the contact to be promoted to LO (as was found for the light neutrino exchange diagrams in Ref. [26]). While computing the $NNNNee$ contact interaction will prove challenging, it is, in principle, calculable with current technology and resources [110]. Finally, in order to disentangle long- and short-range $0\nu\beta\beta$ effects, investigation of quenching of the axial coupling g_A in multinucleon systems [111–113], as well as the isotensor axial polarizability [114,115], will also be useful.

Our results can, in principle, be used to determine contributions from any BSM model leading to short-range $0\nu\beta\beta$ to leading order in χPT. However, these results must first be incorporated into nuclear physics models capable of describing large nuclei. Currently, there is sizable discrepancy between different models and uncertainty quantification remains difficult, challenges that will need to be overcome in order to faithfully connect experiment with theory.

We thank Emanuele Mereghetti and Vincenzo Cirigliano for helpful conversations and correspondence and Emanuele for pointing out a mistake in our original chiral extrapolation formulas. Numerical calculations were performed with the CHROMA software suite [116] with QUDA inverters [117,118] on Surface at LLNL, supported by the LLNL Multiprogrammatic and Institutional Computing program through a Tier 1 Grand Challenge award, and on Titan, a resource of the Oak Ridge Leadership Computing Facility at the Oak Ridge National Laboratory, which is supported by the Office of Science of the U.S. Department of Energy under Award No. DE-AC05-00OR22725, through an INCITE award. The calculations were efficiently interleaved with those in Ref. [41–43] using METAQ [119]. This work was supported by the NVIDIA Corporation (MAC), DFG, and NSFC through funds provided to the Sino-German CRC 110 "Symmetries and the Emergence of Structure in QCD" (E. B.), a RIKEN SPDR fellowship (E. R.), the Leverhulme Trust (N. G.), the U.S. Department of Energy, Office of Science: Office of Nuclear Physics (E. B., D. A. B., C. C. C., T. K., H. M. C., A. N., E. R., B. J., P. V., A. W. L.); Office of Advanced Scientific Computing (E. B., B. J., T. K., A. W. L.); Nuclear Physics Double Beta Decay Topical Collaboration (D. A. B., H. M. C., A. W. L., A. N.); the DOE Early Career Award Program (D. A. B., C. C. C., H. M. C., A. W. L.); and the LLNL Livermore Graduate Scholar Program (D. A. B.). This work was performed under the auspices of the U.S. Department of Energy by LLNL under Award No. DE-AC52-07NA27344 (E. B., E. R., P. V.), and by LBNL under Award No. DE-AC02-05CH11231, under which the Regents of the University of California manage and operate LBNL. This research was supported in part by the National Science Foundation under Grant No. NSF PHY15-15738 (B. C. T.) and NSF PHY-1748958, and parts of this work were completed at the program "Frontiers in Nuclear Physics" (NUCLEAR16).

*annichol@email.unc.edu

[1] J. Schechter and J. W. F. Valle, Neutrinoless double-β decay in $\mathrm{SU}(2) \times \mathrm{U}(1)$ theories, Phys. Rev. D 25, 2951 (1982).

[2] M. Hirsch, S. Kovalenko, and I. Schmidt, Extended black box theorem for lepton number and flavor violating processes, Phys. Lett. B **642**, 106 (2006).

[3] S. Pascoli, S. T. Petcov, and A. Riotto, Leptogenesis and low energy *CP* violation in neutrino physics, Nucl. Phys. **B774**, 1 (2007).

[4] S. Davidson, E. Nardi, and Y. Nir, Leptogenesis, Phys. Rep. **466**, 105 (2008).

[5] M. Agostini *et al.*, Background-free search for neutrinoless double-β decay of ^{76}Ge with GERDA, Nature (London) **544**, 47 (2017).

[6] S. Andringa *et al.* (SNO+Collaboration), Current status and future prospects of the SNO+experiment, Adv. High Energy Phys. **2016**, 6194250 (2016).

[7] S. R. Elliott *et al.*, Initial results from the Majorana Demonstrator, J. Phys. Conf. Ser. **888**, 012035 (2017).

[8] A. Gando *et al.* (KamLAND-Zen Collaboration), Limit on Neutrinoless $\beta\beta$ Decay of ^{136}Xe from the First Phase of KamLAND-Zen and Comparison with the Positive Claim in ^{76}Ge, Phys. Rev. Lett. **110**, 062502 (2013).

[9] M. Agostini *et al.* (GERDA Collaboration), Results on Neutrinoless Double-β Decay of ^{76}Ge from Phase I of the GERDA Experiment, Phys. Rev. Lett. **111**, 122503 (2013).

[10] J. B. Albert *et al.* (EXO-200 Collaboration), Search for Majorana neutrinos with the first two years of EXO-200 data, Nature (London) **510**, 229 (2014).

[11] C. Alduino *et al.* (CUORE Collaboration), First Results from CUORE: A Search for Lepton Number Violation via $0\nu\beta\beta$ Decay of ^{130}Te, Phys. Rev. Lett. **120**, 132501 (2018).

[12] K. Han (PandaX-III Collaboration), PandaX-III: Searching for neutrinoless double beta decay with high pressure gaseous time projection chambers, in *Proceedings of the 15th International Conference on Topics in Astroparticle and Underground Physics (TAUP 2017) Sudbury, Ontario, Canada, 2017* (2017), http://inspirehep.net/record/1632173.

[13] O. Azzolini *et al.* (CUPID-0 Collaboration), First Result on the Neutrinoless Double-β Decay of ^{82}Se with CUPID-0, Phys. Rev. Lett. **120**, 232502 (2018).

[14] J. B. Albert *et al.* (EXO Collaboration), Search for Neutrinoless Double-Beta Decay with the Upgraded EXO-200 Detector, Phys. Rev. Lett. **120**, 072701 (2018).

[15] K. Alfonso *et al.* (CUORE Collaboration), Search for Neutrinoless Double-Beta Decay of ^{130}Te with CUORE-0, Phys. Rev. Lett. **115**, 102502 (2015).

[16] A. Gando *et al.* (KamLAND-Zen Collaboration), Search for Majorana Neutrinos near the Inverted Mass Hierarchy Region with KamLAND-Zen, Phys. Rev. Lett. **117**, 082503 (2016); Erratum, Phys. Rev. Lett. **117**, 109903 (E) (2016).

[17] M. Gell-Mann, P. Ramond, and R. Slansky, Complex spinors and unified theories, in *Proceedings of the Supergravity Workshop Stony Brook, New York, 1979* [Conf. Proc. C790927, 315 (1979)].

[18] T. Yanagida, Horizontal symmetry and masses of neutrinos, in *Proceedings of the Workshop on the Unified Theories and the Baryon Number in the Universe, Tsukuba, Japan, 1979* [Conf. Proc. C7902131, 95 (1979)].

[19] S. L. Glashow, The future of elementary particle physics, in *Quarks and Leptons*, edited by M. Lévy, J.- L. Basdevant, D. Speiser, J. Weyers, R. Gastmans, and M. Jacob (Springer, Boston, Massachusetts, 1980) p. 687.

[20] R. N. Mohapatra and G. Senjanović, Neutrino Mass and Spontaneous Parity Nonconservation, Phys. Rev. Lett. **44**, 912 (1980).

[21] P. Ramond, The family group in grand unified theories, in *Proceedings of the International Symposium on Fundamentals of Quantum Theory and Quantum Field Theory Palm Coast, Florida, 1979* (1979) p. 265, http://inspirehep.net/record/140422.

[22] G. Prezeau, M. Ramsey-Musolf, and P. Vogel, Neutrinoless double beta decay and effective field theory, Phys. Rev. D **68**, 034016 (2003).

[23] M. L. Graesser, An electroweak basis for neutrinoless double β decay, J. High Energy Phys. 08 (2017) 099.

[24] S. Weinberg, Effective chiral Lagrangians for nucleon-pion interactions and nuclear forces, Nucl. Phys. **B363**, 3 (1991).

[25] S. Weinberg, Nuclear forces from chiral Lagrangians, Phys. Lett. B **251**, 288 (1990).

[26] V. Cirigliano, W. Dekens, J. de Vries, M. L. Graesser, E. Mereghetti, S. Pastore, and U. van Kolck, New Leading Contribution to Neutrinoless Double-β Decay, Phys. Rev. Lett. **120**, 202001 (2018).

[27] G. Peter Lepage, The Analysis of Algorithms for Lattice Field Theory, 97 (1989), http://inspirehep.net/record/287173/.

[28] L. Lellouch and M. Luscher, Weak transition matrix elements from finite volume correlation functions, Commun. Math. Phys. **219**, 31 (2001).

[29] R. A. Briceño and M. T. Hansen, Relativistic, model-independent, multichannel $2 \to 2$ transition amplitudes in a finite volume, Phys. Rev. D **94**, 013008 (2016).

[30] Y. Takahashi, The Fierz identities, in *Progress in Quantum Field Theory*, edited by H. Ezawa and S. Kamefuchi (North-Holland, Amsterdam, 1986) p. 121.

[31] E. Follana, Q. Mason, C. Davies, K. Hornbostel, G. P. Lepage, J. Shigemitsu, H. Trottier, and K. Wong (HPQCD and UKQCD Collaborations), Highly improved staggered quarks on the lattice, with applications to charm physics, Phys. Rev. D **75**, 054502 (2007).

[32] A. Bazavov, C. Bernard, J. Komijani, C. DeTar, L. Levkova, W. Freeman, S. Gottlieb, R. Zhou, U. M. Heller, J. E. Hetrick, J. Laiho, J. Osborn, R. L. Sugar, D. Toussaint, and R. S. Van de Water (MILC Collaboration), Lattice QCD ensembles with four flavors of highly improved staggered quarks, Phys. Rev. D **87**, 054505 (2013).

[33] A. Bazavov, C. Bernard, N. Brown, J. Komijani, C. DeTar, J. Foley, L. Levkova, S. Gottlieb, U. M. Heller, J. Laiho, R. L. Sugar, D. Toussaint, and R. S. Van de Water (MILC Collaboration), Gradient flow and scale setting on MILC HISQ ensembles, Phys. Rev. D **93**, 094510 (2016).

[34] R. C. Brower, H. Neff, and K. Orginos, Mobius fermions: Improved domain wall chiral fermions, Nucl. Phys. B, Proc. Suppl. **140**, 686 (2005).

[35] R. C. Brower, H. Neff, and K. Orginos, Mobius fermions, Nucl. Phys. B, Proc. Suppl. **153**, 191 (2006).

[36] R. C. Brower, H. Neff, and K. Orginos, The Möbius domain wall fermion algorithm, Comput. Phys. Commun. **220**, 1 (2017).

[37] R. Narayanan and H. Neuberger, Infinite N phase transitions in continuum Wilson loop operators, J. High Energy Phys. 03 (2006) 064.
[38] M. Luscher and P. Weisz, Perturbative analysis of the gradient flow in non-abelian gauge theories, J. High Energy Phys. 02 (2011) 051.
[39] M. Luscher, Chiral symmetry and the Yang–Mills gradient flow, J. High Energy Phys. 04 (2013) 123.
[40] E. Berkowitz, C. Bouchard, C. C. Chang, M. A. Clark, B. Joó, T. Kurth, C. Monahan, A. Nicholson, K. Orginos, E. Rinaldi, P. Vranas, and A. Walker-Loud, Möbius domain-wall fermions on gradient-flowed dynamical HISQ ensembles, Phys. Rev. D **96**, 054513 (2017).
[41] E. Berkowitz, D. Brantley, C. Bouchard, C. C. Chang, M. A. Clark, N. Garron, B. Joó, T. Kurth, C. Monahan, H. Monge-Camacho, A. Nicholson, K. Orginos, E. Rinaldi, P. Vranas, and A. Walker-Loud, An accurate calculation of the nucleon axial charge with lattice QCD, arXiv:1704.01114.
[42] C. C. Chang, A. Nicholson, E. Rinaldi, E. Berkowitz, N. Garron, D. Brantley, H. Monge-Camacho, C. Monahan, C. Bouchard, M. A. Clark, B. Joó, T. Kurth, K. Orginos, P. Vranas, and A. Walker-Loud, Nucleon axial coupling from lattice QCD, EPJ Web Conf. **175**, 01008 (2018).
[43] C. C. Chang, A. Nicholson, E. Rinaldi, E. Berkowitz, N. Garron, D. Brantley, H. Monge-Camacho, C. Monahan, C. Bouchard, M. A. Clark, B. Joó, T. Kurth, K. Orginos, P. Vranas, and A. Walker-Loud, A percent-level determination of the nucleon axial coupling from quantum chromodynamics, Nature (London) **558**, 91 (2018).
[44] Y. Aoki *et al.*, Continuum limit of B_K from $2+1$ flavor domain wall QCD, Phys. Rev. D **84**, 014503 (2011).
[45] S. Durr *et al.*, Precision computation of the kaon bag parameter, Phys. Lett. B **705**, 477 (2011).
[46] P. A. Boyle, N. Garron, and R. J. Hudspith (RBC and UKQCD Collaborations), Neutral kaon mixing beyond the standard model with $n_f = 2+1$ chiral fermions, Phys. Rev. D **86**, 054028 (2012).
[47] V. Bertone *et al.* (ETM Collaboration), Kaon mixing beyond the SM from $N_f = 2$ tmQCD and model independent constraints from the UTA, J. High Energy Phys. 03 (2013) 089; Erratum, J. High Energy Phys. 07 (2013) 143(E).
[48] T. Bae *et al.* (SWME Collaboration), Neutral kaon mixing from new physics: Matrix elements in $N_f = 2+1$ lattice QCD, Phys. Rev. D **88**, 071503 (2013).
[49] T. Bae *et al.* (SWME Collaboration), Improved determination of BK with staggered quarks, Phys. Rev. D **89**, 074504 (2014).
[50] N. Carrasco, P. Dimopoulos, R. Frezzotti, V. Lubicz, G. C. Rossi, S. Simula, and C. Tarantino (ETM Collaboration), $\Delta S = 2$ and $\Delta C = 2$ bag parameters in the standard model and beyond from $N_f = 2+1+1$ twisted-mass lattice QCD, Phys. Rev. D **92**, 034516 (2015).
[51] B. J. Choi *et al.* (SWME Collaboration), Kaon BSM B-parameters using improved staggered fermions from $N_f = 2+1$ unquenched QCD, Phys. Rev. D **93**, 014511 (2016).
[52] N. Garron, R. J. Hudspith, and A. T. Lytle (RBC and UKQCD Collaborations), Neutral kaon mixing beyond the standard model with $n_f = 2+1$ chiral fermions part 1: Bare matrix elements and physical results, J. High Energy Phys. 11 (2016) 001.
[53] A. Bazavov *et al.*, Short-distance matrix elements for D^0-meson mixing for $N_f = 2+1$ lattice QCD, Phys. Rev. D **97**, 034513 (2018).
[54] E. Gamiz, C. T. H. Davies, G. P. Lepage, J. Shigemitsu, and M. Wingate (HPQCD Collaboration), Neutral B meson mixing in unquenched lattice QCD, Phys. Rev. D **80**, 014503 (2009).
[55] N. Carrasco *et al.* (ETM Collaboration), B-physics from $N_f = 2$ tmQCD: The standard model and beyond, J. High Energy Phys. 03 (2014) 016.
[56] Y. Aoki, T. Ishikawa, T. Izubuchi, C. Lehner, and A. Soni, Neutral B meson mixings and B meson decay constants with static heavy and domain-wall light quarks, Phys. Rev. D **91**, 114505 (2015).
[57] A. Bazavov *et al.* (Fermilab Lattice and MILC Collaborations), $B^0_{(s)}$-mixing matrix elements from lattice QCD for the standard model and beyond, Phys. Rev. D **93**, 113016 (2016).
[58] M. I. Buchoff, C. Schroeder, and J. Wasem, Neutron-antineutron oscillations on the lattice, Proc. Sci., LATTICE2012 (**2012**) 128 [arXiv:1207.3832].
[59] S. Syritsyn, M. I. Buchoff, C. Schroeder, and J. Wasem, Neutron-antineutron oscillation matrix elements with domain wall fermions at the physical point, Proc. Sci., LATTICE2015 (**2015**) 132.
[60] E. Rinaldi, S. Syritsyn, M. L. Wagman, M. I. Buchoff, C. Schroeder, and J. Wasem, Neutron-antineutron oscillations from lattice QCD, arXiv:1809.00246.
[61] A. Nicholson, E. Berkowitz, C. C. Chang, M. A. Clark, B. Joó, T. Kurth, E. Rinaldi, B. Tiburzi, P. Vranas, and A. Walker-Loud, Neutrinoless double beta decay from lattice QCD, Proc. Sci., LATTICE2016 (**2016**) 017 [arXiv:1608.04793].
[62] See Supplemental Material at http://link.aps.org/supplemental/10.1103/PhysRevLett.121.172501 for detailed discussion about nonperturbative renormalization, the derivation of the chiral extrapolation formulae, studies of excited state contamination, an uncertainty breakdown, and results for the associated low-energy constants and related pion bag parameter, B_π, which includes Refs. [63–83].
[63] A. J. Buras, M. Misiak, and J. Urban, Two loop QCD anomalous dimensions of flavor changing four quark operators within and beyond the standard model, Nucl. Phys. **B586**, 397 (2000).
[64] T. van Ritbergen, J. A. M. Vermaseren, and S. A. Larin, The four loop beta function in quantum chromodynamics, Phys. Lett. B **400**, 379 (1997).
[65] K. G. Chetyrkin, B. A. Kniehl, and M. Steinhauser, Strong Coupling Constant with Flavor Thresholds at Four Loops in the MS Scheme, Phys. Rev. Lett. **79**, 2184 (1997).
[66] O. Bar, G. Rupak, and N. Shoresh, Simulations with different lattice dirac operators for valence and sea quarks, Phys. Rev. D **67**, 114505 (2003).
[67] O. Bar, G. Rupak, and N. Shoresh, Chiral perturbation theory at $O(a^2)$ for lattice QCD, Phys. Rev. D **70**, 034508 (2004).
[68] B. C. Tiburzi, Baryon masses at $O(a^2)$ in chiral perturbation theory, Nucl. Phys. **A761**, 232 (2005).

[69] O. Bar, C. Bernard, G. Rupak, and N. Shoresh, Chiral perturbation theory for staggered sea quarks and Ginsparg-Wilson valence quarks, Phys. Rev. D **72**, 054502 (2005).

[70] B. C. Tiburzi, Baryons with Ginsparg-Wilson quarks in a staggered sea, Phys. Rev. D **72**, 094501 (2005); Erratum, Phys. Rev. D **79**, 039904(E) (2009).

[71] J.-W. Chen, D. O'Connell, R. S. Van de Water, and A. Walker-Loud, Ginsparg-Wilson pions scattering on a staggered sea, Phys. Rev. D **73**, 074510 (2006).

[72] J.-W. Chen, D. O'Connell, and A. Walker-Loud, Two meson systems with Ginsparg-Wilson valence quarks, Phys. Rev. D **75**, 054501 (2007).

[73] J.-W. Chen, D. O'Connell, and A. Walker-Loud, Universality of mixed action extrapolation formulae, J. High Energy Phys. 04 (2009) 090.

[74] J.-W. Chen, M. Golterman, D. O'Connell, and A. Walker-Loud, Mixed action effective field theory: An addendum, Phys. Rev. D **79**, 117502 (2009).

[75] C. W. Bernard and M. F. L. Golterman, Partially quenched gauge theories and an application to staggered fermions, Phys. Rev. D **49**, 486 (1994).

[76] S. R. Sharpe, Enhanced chiral logarithms in partially quenched QCD, Phys. Rev. D **56**, 7052 (1997); Erratum, Phys. Rev. D **62**, 099901(E) (2000).

[77] S. R. Sharpe and N. Shoresh, Physical results from unphysical simulations, Phys. Rev. D **62**, 094503 (2000).

[78] S. R. Sharpe and N. Shoresh, Partially quenched chiral perturbation theory without Φ_0, Phys. Rev. D **64**, 114510 (2001).

[79] C. Bernard and M. Golterman, On the foundations of partially quenched chiral perturbation theory, Phys. Rev. D **88**, 014004 (2013).

[80] J. Noaki *et al.* (TWQCD and JLQCD Collaborations), Convergence of the Chiral Expansion in Two-Flavor Lattice QCD, Phys. Rev. Lett. **101**, 202004 (2008).

[81] S. Aoki *et al.*, Review of lattice results concerning low-energy particle physics, Eur. Phys. J. C **77**, 112 (2017).

[82] S. Borsanyi *et al.*, High-precision scale setting in lattice QCD, J. High Energy Phys. 09 (2012) 010.

[83] C. Patrignani *et al.* (Particle Data Group), Review of particle physics, Chin. Phys. C **40**, 100001 (2016).

[84] J. Gasser and H. Leutwyler, Chiral perturbation theory to one loop, Ann. Phys. (N.Y.) **158**, 142 (1984).

[85] S. R. Sharpe and R. L. Singleton, Jr., Spontaneous flavor and parity breaking with Wilson fermions, Phys. Rev. D **58**, 074501 (1998).

[86] J. Gasser and H. Leutwyler, Spontaneously broken symmetries: Effective Lagrangians at finite volume, Nucl. Phys. **B307**, 763 (1988).

[87] G. Martinelli, C. Pittori, C. T. Sachrajda, M. Testa, and A. Vladikas, A general method for nonperturbative renormalization of lattice operators, Nucl. Phys. **B445**, 81 (1995).

[88] C. Sturm, Y. Aoki, N. H. Christ, T. Izubuchi, C. T. C. Sachrajda, and A. Soni (RBC and UKQCD Collaborations), Renormalization of quark bilinear operators in a momentum-subtraction scheme with a nonexceptional subtraction point, Phys. Rev. D **80**, 014501 (2009).

[89] P. A. Boyle, N. Garron, R. J. Hudspith, C. Lehner, and A. T. Lytle (RBC and UKQCD Collaborations), Neutral kaon mixing beyond the standard model with $n_f = 2 + 1$ chiral fermions. Part 2: Non perturbative renormalisation of the $\Delta F = 2$ four-quark operators, J. High Energy Phys. 10 (2017) 054.

[90] M. Gockeler, R. Horsley, H. Oelrich, H. Perlt, D. Petters, P. E. L. Rakow, A. Schäfer, G. Schierholz, and A. Schiller, Nonperturbative renormalization of composite operators in lattice QCD, Nucl. Phys. **B544**, 699 (1999).

[91] R. Arthur and P. A. Boyle (RBC and UKQCD Collaborations), Step scaling with off-shell renormalisation, Phys. Rev. D **83**, 114511 (2011).

[92] R. Arthur, P. A. Boyle, N. Garron, C. Kelly, and A. T. Lytle (RBC and UKQCD Collaborations), Opening the Rome-Southampton window for operator mixing matrices, Phys. Rev. D **85**, 014501 (2012).

[93] https://github.com/callat-qcd/project_0vbb.

[94] G. P. Lepage, `lsqfit` v9.3 (2018).

[95] V. Cirigliano, W. Dekens, M. Graesser, and E. Mereghetti, Neutrinoless double beta decay and chiral $SU(3)$, Phys. Lett. B **769**, 460 (2017).

[96] A. Pich and E. De Rafael, K anti-K mixing in the standard model, Phys. Lett. **158B**, 477 (1985).

[97] A. Pich and E. de Rafael, Four quark operators and non-leptonic weak transitions, Nucl. Phys. **B358**, 311 (1991).

[98] S. Peris and E. de Rafael, K^0 anti-K^0 mixing in the $1/N_c$ expansion, Phys. Lett. B **490**, 213 (2000).

[99] H. Päs, M. Hirsch, H. V. Klapdor-Kleingrothaus, and S. G. Kovalenko, Towards a superformula for neutrinoless double beta decay, Phys. Lett. B **453**, 194 (1999).

[100] H. Pas, M. Hirsch, H. V. Klapdor-Kleingrothaus, and S. G. Kovalenko, A superformula for neutrinoless double beta decay. 2. The short range part, Phys. Lett. B **498**, 35 (2001).

[101] W. Rodejohann, Neutrino-less double beta decay and particle physics, Int. J. Mod. Phys. E **20**, 1833 (2011).

[102] T. Peng, M. J. Ramsey-Musolf, and P. Winslow, TeV lepton number violation: From neutrinoless double-β decay to the LHC, Phys. Rev. D **93**, 093002 (2016).

[103] S.-F. Ge, M. Lindner, and S. Patra, New physics effects on neutrinoless double beta decay from right-handed current, J. High Energy Phys. 10 (2015) 077.

[104] J. Engel and J. Menéndez, Status and future of nuclear matrix elements for neutrinoless double-beta decay: A review, Rep. Prog. Phys. **80**, 046301 (2017).

[105] F. Ahmed, A. Neacsu, and M. Horoi, Interference between light and heavy neutrinos for $0\nu\beta\beta$ decay in the left-right symmetric model, Phys. Lett. B **769**, 299 (2017).

[106] M. Horoi and A. Neacsu, Towards an effective field theory approach to the neutrinoless double-beta decay, arXiv:1706.05391.

[107] V. Cirigliano, W. Dekens, J. de Vries, M. L. Graesser, and E. Mereghetti, Neutrinoless double beta decay in chiral effective field theory: Lepton number violation at dimension seven, J. High Energy Phys. 12 (2017) 082.

[108] J. Menéndez, Neutrinoless $\beta\beta$ decay mediated by the exchange of light and heavy neutrinos: The role of nuclear structure correlations, J. Phys. G **45**, 014003 (2018).

[109] M. González, S. G. Kovalenko, and M. Hirsch, QCD running in neutrinoless double beta decay: Short-range mechanisms, Phys. Rev. D **93**, 013017 (2016).

[110] T. Kurth, E. Berkowitz, E. Rinaldi, P. Vranas, A. Nicholson, M. Strother, and A. Walker-Loud, Nuclear parity violation from lattice QCD, Proc. Sci., LATTICE2015 (**2015**) 329.

[111] M. J. Savage, P. E. Shanahan, B. C. Tiburzi, M. L. Wagman, F. Winter, S. R. Beane, E. Chang, Z. Davoudi, W. Detmold, and K. Orginos, Axial-current matrix elements in light nuclei from lattice QCD, Proc. Sci., ICHEP2016 (**2016**) 506 [arXiv:1611.00344].

[112] M. J. Savage, P. E. Shanahan, B. C. Tiburzi, M. L. Wagman, F. Winter, S. R. Beane, E. Chang, Z. Davoudi, W. Detmold, and K. Orginos, Proton-Proton Fusion and Tritium β Decay from Lattice Quantum Chromodynamics, Phys. Rev. Lett. **119**, 062002 (2017).

[113] E. Chang, Z. Davoudi, W. Detmold, A. S. Gambhir, K. Orginos, M. J. Savage, P. E. Shanahan, M. L. Wagman, and F. Winter, Nuclear Modification of Scalar, Axial and Tensor Charges from Lattice QCD, Phys. Rev. Lett. **120**, 152002 (2018).

[114] B. C. Tiburzi, M. L. Wagman, F. Winter, E. Chang, Z. Davoudi, W. Detmold, K. Orginos, M. J. Savage, and P. E. Shanahan, Double-β decay matrix elements from lattice quantum chromodynamics, Phys. Rev. D **96**, 054505 (2017).

[115] P. E. Shanahan, B. C. Tiburzi, M. L. Wagman, F. Winter, E. Chang, Z. Davoudi, W. Detmold, K. Orginos, and M. J. Savage, Isotensor Axial Polarizability and Lattice QCD Input for Nuclear Double-β Decay Phenomenology, Phys. Rev. Lett. **119**, 062003 (2017).

[116] R. G. Edwards and B. Joó (SciDAC, LHPC, and UKQCD Collaborations), The chroma software system for lattice QCD, Nucl. Phys. B, Proc. Suppl. **140**, 832 (2005).

[117] M. A. Clark, R. Babich, K. Barros, R. C. Brower, and C. Rebbi, Solving lattice QCD systems of equations using mixed precision solvers on GPUs, Comput. Phys. Commun. **181**, 1517 (2010).

[118] R. Babich, M. A. Clark, B. Joó, G. Shi, R. C. Brower, and S. Gottlieb, Scaling lattice QCD beyond 100 GPUs, in *Proceedings of the SC11 International Conference for High Performance Computing, Networking, Storage and Analysis Seattle, Washington, 2011* (ACM, New York, 2011), doi: 10.1145/2063384.2063478.

[119] E. Berkowitz, METAQ: Bundle supercomputing tasks, arXiv:1702.06122;E. Berkowitz, G. R. Jansen, K. McElvain, and A. Walker-Loud, Job management and task bundling, EPJ Web Conf. **175**, 09007 (2018).